Localisation Techniques to Improve Analysis for BCI

Rianne Hupse
Supervisors: Dr. ir. P. Desain and Prof. dr. C. Gielen

Music, Mind and Machine group, NICI, Radboud University Nijmegen

An experiment is described to explore the possibility to elaborate a new type of brain computer interface (BCI) system: a system in which selective attention to rhythmic tactile stimuli is used to control an external device. It is known that temporal rhythmic tactile stimuli induce a steady-state somatosensory evoked potential oscillating at the same temporal frequency as the driving stimulus. The amplitude of this oscillation increases when the subject is attending to the stimulus. This attention induced power gain can be detected in the EEG (electroencephalogram) and might be translated into commands for a computer or other device. Because EEG data has a small signal to noise ratio, it is investigated if a beamformer spatial filter improves the classification success rates. To be sure that the beamformer filter allocates activity to the correct anatomical locations, a new method is proposed to construct realistic head models. During the experiment, tactile stimuli with different temporal frequencies are presented to the left and right index finger of a subject. The subject is instructed to attend to one finger and to ignore the sensations of the other finger. Perception conditions, in which only one finger was stimulated, were included as a baseline. Single trial EEG and voxel data was used in a classification algorithm to detect which finger was attended. Classification rates are relatively high (± 90%) for perception conditions, while selective attention conditions give success rates below chance level. An explanation for this can be that the attention induced power gain is too small to be detected in single trials. Results show that beamforming allocates the frequencies presented to left and right index finger to separate areas of the brain. This is in contrast to electrode data, in which the two frequencies reach electrodes at both sides of the scalp. Therefore, by using the beamformer filter the power of a single stimulus is focused to a single area which will increase the signal to noise ratio. However, classification success rates show no improvements when the beamformer filter is used. A suggestion for further research is to include a discrimination task in the experiment which might increase the attention level of the subject and therefore the attention induced power gain. The amount of trials can be increased that is used as a training set in the cross validation procedure of the classification algorithm. Furthermore, the amount of trials used for estimating the covariance between the sensors, which is necessary for building the beamformer filter, might im- prove the results. More experiments are necessary to investigate if the results described here are representative to sessions with other subjects.

1.Introduction

1.1 Brain Computer Interfaces

Patients suffering from motor diseases can have difficulties performing even the simplest actions. One example is amyotrophic lateral sclerosis (ALS), a disease in which a progressive degeneration of motor neurons leads to an inability of the brain to control movements. In the later stage of this disease patients may become totally paralyzed. Other examples of motor diseases are brainstem stroke, brain or spinal cord injury and multiple sclerosis. In most cases only motor functions are affected; patients do not experience impaired intellectual reasoning, vision or hearing.

A system in which an external device like a speech synthesizer, a computer or a wheelchair can be controlled without the usage of muscles would greatly improve the quality of life of these patients. For this reason brain computer interfaces (BCI) are being developed. Using these interfaces a patient will be able to control a device using his/her brain only, for example by directing his/her attention to one of multiple stimuli present. While controlling the device, the patient is wearing an electrode cap for measuring the electrocortical encephalogram (EEG) signals. A basic design for a BCI system is showed in figure 1.1. Signals are measured by electrodes at the scalp or at the surface of the brain. Specific features are extracted from the digitized signal. A translation algorithm makes a decision based on these features. This decision is executed by sending commands to the external device like a typing device, a wheelchair or hand prothesis. The loop is closed by the subject who is observing the device. In this way the subject can learn to adapt to the system.

Besides EEG, there are multiple other techniques available to measure activity from the brain such as magnetoencephalography (MEG), positron emission tomography (PET), functional magnetic resonance imaging (fMRI), and optical imaging. However, these techniques require expensive equipment that cannot be used in every environment. Furthermore, fMRI and optical imaging are slow and are therefore not suitable for a device that has to measure quickly changing patterns of mental activity. Because EEG measurement has a high time resolution and requires simple and inexpensive equipment, it might be the most suitable technique to be used in bci systems.

1.2 History of Brain Computer Interfaces

The first BCI studies started with research in monkeys. Electrodes were implanted into the brain of a monkey and firing patterns were measured of individual and groups of neurons. In 1973 the group of Fetz found that macaque monkeys were able to selectively adjust the firing rate of individual cortical neurons to attain a particular level of cell activity. This was done by the use of a conditioning paradigm and providing sensory feedback that signaled the level of neuronal firing [7]. Based on these findings, Schmidt proposed in 1980 that activity measured in cortical motor centers might be used to activate external devices [20].

In 2000 Nicolelis developed a BCI system that recorded brain activity from implanted electrodes in monkeys. This activity was used to control a robot arm [4] [24]. In this system, several motor parameters such as velocity, gripping force and hand position were extracted from the neural firing patterns of different motor areas. The robot arm was invisible to the monkeys, but feedback of the movements was provided by a visual display. During training, the performance of the monkeys improved. Control of the robot arm was even possible when the arms of the monkeys did not move.

Another group that measured neural activity in monkeys is the group of Andersen. Activity was measured while the monkey was preparing to reach to a stimulus that was shown before. Using activity patterns collected in these training trials, it was possible to predict the reach direction of the monkey in other trials [16].

The use of implanted electrodes provides a way to obtain signals from the brain with a high signal to noise ratio. However, this invasive technique is not well suited for use in human BCI systems. Therefore techniques were developed to control a device using the signals measured from the scalp: EEG signals. Because of a lower signal to noise ratio and the fact that an EEG electrode measures signals coming from a huge amount of neurons together, other features in the signal are extracted than in the case of implanted electrodes. Systems that use EEG signals can be divided into three groups: systems using mu and beta rhythms, systems using slow cortical potentials and systems using P300 evoked potentials.

One of the groups that uses mu and beta rhythms for BCI is the group of Pfurtscheller. Knowledge about beta and gamma synchronization

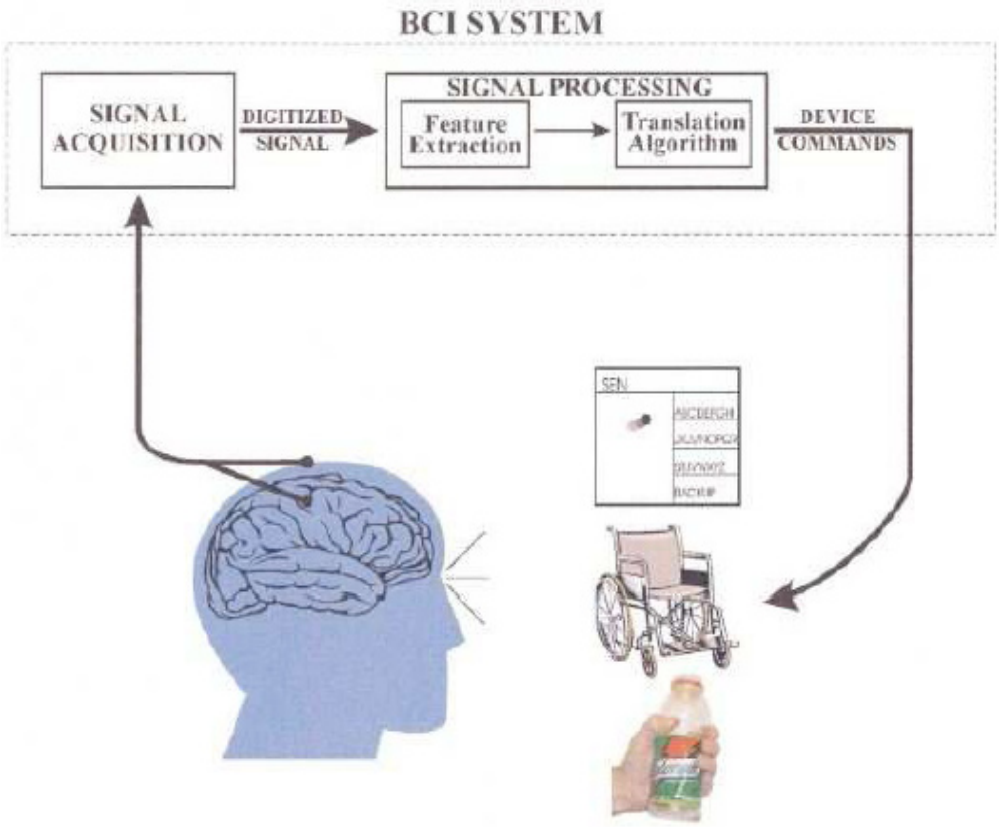

Figure 1.1: Basic design of a BCI system, adopted from [25].

in the human brain during the imagination of simple motor tasks was used to control several devices like a virtual keyboard device and an orthotic device that opens and closes a paralyzed hand [18] [19].

A group that uses slow cortical potentials, is the group of Birbaumer. Slow cortical potentials (SCPs) are slow voltage changes generated in the cortex that occur over a time period of 0.5 to 10 seconds. Negative scps are associated with functions involving cortical activation, while positive scps are associated with reduced cortical activation [2]. It has been shown that subjects can control these potentials and thereby control a cursor on a computer screen [3]. However, the training period lasts for several months and is very demanding for the patient.

Besides mu and gamma rhythms and slow cortical potentials, P300 evoked potentials can be used for BCI. A P300 evoked potential is the positive peak in the EEG that is measured over parietal cortex about 300 ms after an auditory, visual or somatosensory stimulus is presented to a subject [6]. Donchin uses this P300 response in a paradigm in which a 6 by 6 matrix of letters is presented to a subject, which has to attend to one letter. Every 125 ms, a row or a column of this matrix flashes. After a set of trials the average P300 amplitude is calculated to the flashing of every row and column. Based on these P300 amplitudes, the system chooses the letter that is located in the row and the column that give the largest mean P300 potential. The advantage of using the P300 amplitude is that it requires no initial user training. However, the P300 response is likely to change over time and over long time periods P300 might habituate.

1.3 The challenge of improving the signal to noise ratio

The biggest challenge of developing brain computer interfaces lies in the fact that the signal to noise ratio of eeg signals is low, which makes recognition of different activity patterns hard. This low signal to noise ratio is due to measurement noise, ongoing brain processes that do not correlate with the relevant mental activity and 'smearing' out of signals by different tissues in the head. In brain research usually the averaging over multiple trials is used to reduce these noise effects. However, in bci this will lead to a considerable increase in classification time because the system has to wait for multiple trials before being able to select an response. When developing a faster interface in

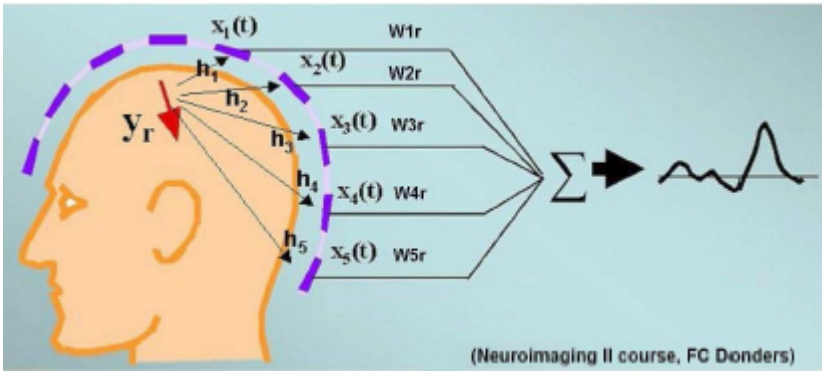

Figure 1.2: The basic principle of beamforming is to construct a forward model H that predicts the measured potentials at the scalp due to a single dipole in the brain. Using this forward model and the covariance between the sensor measurements, a filter is constructed. By multiplying the potentials measured at every sensor by the filter weights and summing the results, the activity at the location of the dipole is calculated. (Figure adopted from the FC Donders Centre.)

which single trials are used, filtering of the signals to obtain a higher signal to noise ratio becomes important. Several temporal filters like bandpass filters and notch filters are used to decrease the noise level in single trial EEG data. Also spatial filters like independent component analysis (ICA) and principal component analysis (PCA) are used to combine the data measured by the different channels in a linear way into signals representing a few 'virtual' channels measuring the independent or principal sources that are active. In this way relevant information is extracted from the data that can be used for classification algorithms. However, these methods do not use any information about the known location and behaviour of active sources in the brain. By including this information in a spatial filter the potentials stemming from certain brain areas can be optimally extracted while potentials from other areas are suppressed. The use of this kind of spatial filters will result in signals that can achieve a neuro-physiological interpretation and might give better results in classification algorithms.

1.4 Beamforming

A localisation technique often used in brain research is called 'beamforming'. In this approach we calculate the activity present in volume units in the brain called voxels (volume pixels) from the signals measured by the electrodes. These signals can be interpreted as stemming from virtual electrodes measuring directly in the brain itself. Therefore there is no 'smearing out' of potentials due to different conductivities of the different tissue layers in between the brain and the electrodes; every virtual electrode measures activity coming from one single voxel. From the set of voxels a subset can be chosen from which the activity patterns over time are used in the classification algorithm. By doing this, we concentrate only on the part of signal that is expected to originate from one or multiple brain areas that are relevant for the processing of the stimuli.

Beamforming roughly consists of constructing a forward model which predicts the potential distribution at the scalp due to activity in a certain voxel. This model is inverted to estimate the activity in this voxel that is related to the measured potential distribution (figure 1.2 adopted from [26]). An example of a resulting activity pattern can be seen in figure 1.3. Beamforming is often used in MEG (magnetoencephalography) research in which the magnetic fields close to the scalp are measured. Because magnetic fields are not affected by the different tissues in the head, the forward model only depends on the shape of the head of the subject. However, for eeg research the construction of the forward model is more complicated. A model of the shape and conductivity of all different tissues in the head is necessary to be able to calculate the potentials measured at the scalp due to activation of a certain brain area. Because it is hard to construct a realistic head model containing the precise shapes and conductivity values of every tissue type, often a simplified model is used. This simplified model usually consists of three compartments for the brain (including cerebral spinal fluid, CSF), skull and scalp. In this model the brain compartment is a sphere and the skull and scalp compartments are two spherical shells around the brain compartment. In order to obtain a more precise locatisation of brain activity we developed head models containing more realistic shapes for the three compartments using MRI (magnetic resonance imaging) scans of

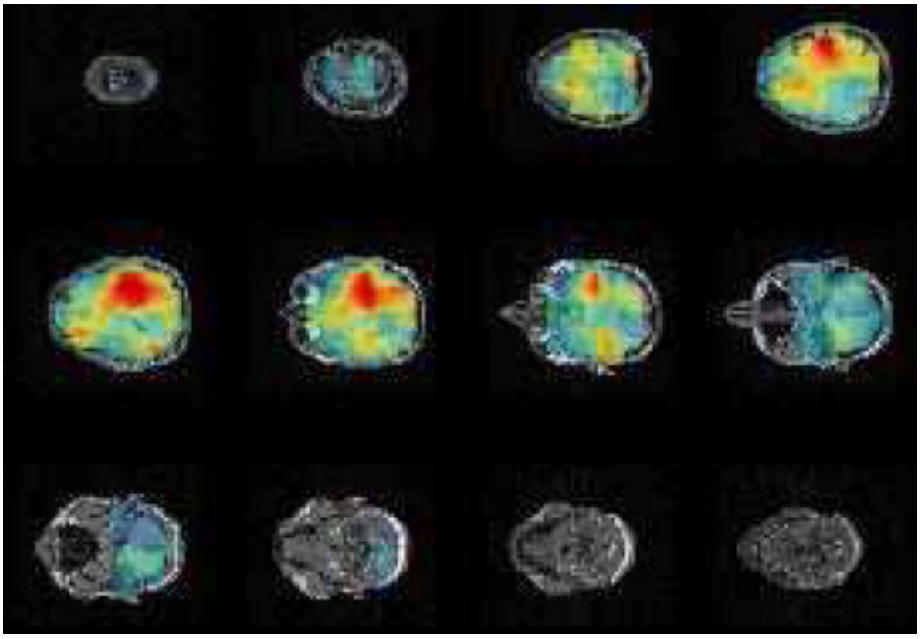

Figure 1.3: Example of brain activity estimated by beamforming. The activity patterns are plotted on top of the slices of the anatomical mri of the subject. Red indicates high brain activity, blue indicates low brain activity. The data set is from a language study on semantically congruent and incongruent sentences. (Image is adopted from the Fieldtrip tutorial of the F.C. Donders Centre for Cognitive Neuroimaging in Nijmegen)

the subjects.

1.5 Our approach

In section 1.2 three different types of BCI systems are described that use EEG measurements. We aim to elaborate a new type of BCI system: a system in which fast temporal rhythms in brain activity are detected that are naturally driven by rhythmic stimuli. When using these naturally occurring features in brain activity for classification the subject does not have to learn to adjust to the system and the training period will be shorter. In our experiments we use vibrotactile stimuli. It is known that vibrotactile stimuli induce a steady-state somatosensory evoked potential. The evoked potential has the same temporal frequency as the driving stimulus [12] [13] [21]. Furthermore it is known that if vibrotactile stimuli with different temporal frequencies are applied simultaneously to the index finger of the left and the right hand, the steady state potential that oscillates in the frequency of the stimulus at the attended finger is enlarged compared to when the other finger is attended [9]. Our goal is to develop a system that is able to select the finger that the subject is attending to, based on the measured EEG signals. By selecting his/her attention, the subject is able to control the output of a computer or a machine, for example a cursor on a screen.

1.6 Overview thesis

In this thesis a BCI experiment is described in which vibrotactile stimuli are used. Because beamforming might improve results in classification algorithms, the measured EEG data is filtered using a beamformer filter. An important aspect of building the beamformer filter is the construction of a model of the different tissues in the head. The methods we used for the construction of a realistic head model are described in section 2.1 and more extended in appendix A. The stimuli we used in the experiment are described in section 2.2. Section 2.3 describes the EEG data acquisition. The analysis section 2.4 consists of the alignment of electrode positions to the anatomical MRI, the construction of the forward model and the analysis of the EEG data including beamforming. The theory of beamforming is described more extended in appendix B. Results are shown in section 3. Section 3.1 shows beamformer activity images for both perception and selective attention conditions. In section 3.2 power differences between contralateral and ipsilateral channels are shown, and in section 3.3 the attention induced power change. Section 3.4 describes the classification success rates for both electrode (not beamformer filtered) and voxel (beamformer filtered) data. Discussion points are given in section 4.

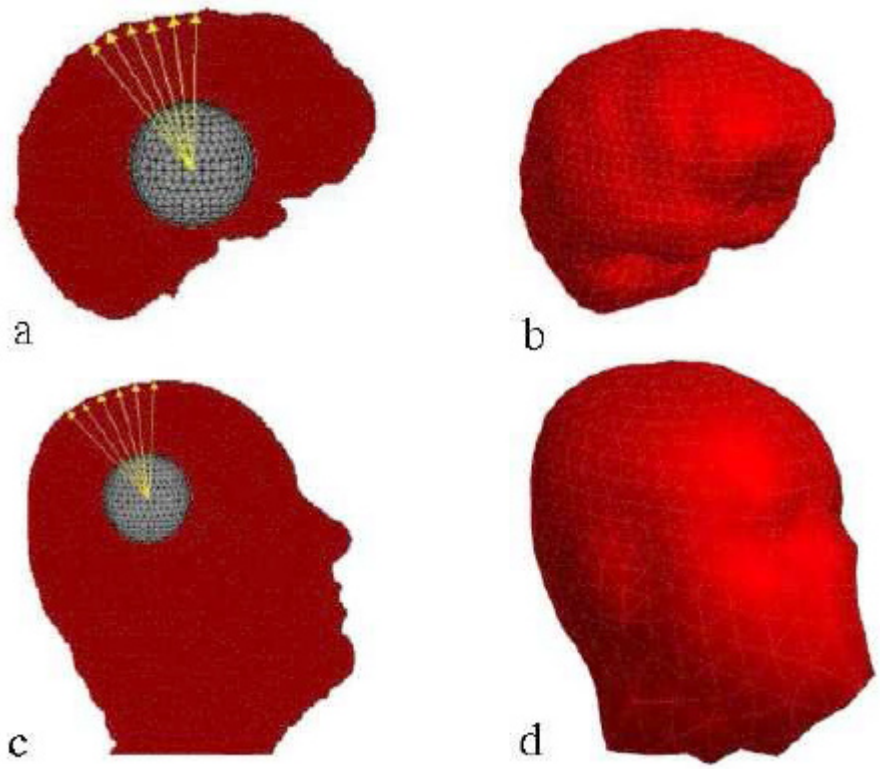

Figure 2.1: a and c: Evenly triangulated sphere at the centre of gravity of the logical brain volume depicted on top of the saggital section of the brain volume (a) and on top of the saggital section of the head volume (c). The vertices of the triangulated sphere were projected onto the outside of the volumes by interpolating lines going from the centre of gravity to the vertices. b and d: Resulting triangulated surfaces representing the outside of the brain and the scalp.

2.Materials and methods

2.1 Construction of realistic head models

To obtain accurate forward models to construct the beamformer filters, we created realistic head models for healthy subjects that participated in the experiments. The head models consisted of three triangulated surfaces representing the outside of the brain, the skull and the scalp compartment. The methods we used for obtaining these surfaces are described in appendix A. A summary of the construction is given in this section.

First, for every subject a T1-weighed (anatomical) mri was made in a 1.5T SIEMENS Sonata scanner. During scanning, subjects wore ear plugs in which vitamin E gel capsules were placed. Vitamin E appears bright on mri scans and can be used as a marker in the alignment of measured sensor coordinates to the MRI.

From the MR scan, the white matter, gray matter and cerebral spinal fluid (CSF) compartment were extracted using the segmentation tool from the Statistical Parameter Mapping software package (SPM) which is a method by Ashburner and Friston [1]. These compartments form together the brain volume. A triangulated surface of this volume is obtained by projecting the vertices of an evenly triangulated sphere onto the outside of the volume (figure 2.1a and b).

The original MRI was thresholded to obtain a volume representing the whole head of the subject. Again vertices of an evenly triangulated sphere were projected onto the outside of this volume to obtain the triangulated surface modeling the outside of the scalp (figure 2.1c and d).

The construction of the surface surrounding the scalp was more difficult than that of the brain and scalp because there was no method to extract the skull volume from an MRI. However, the method we used to create the forward models (the boundary element method) only needed a triangulated surface around the skull volume as input. This means only the boundary points between skull and scalp at the limited number of projection lines were needed instead of the selection of all single voxels being part of the skull. Therefore we combined the segmentation and triangulation into one single

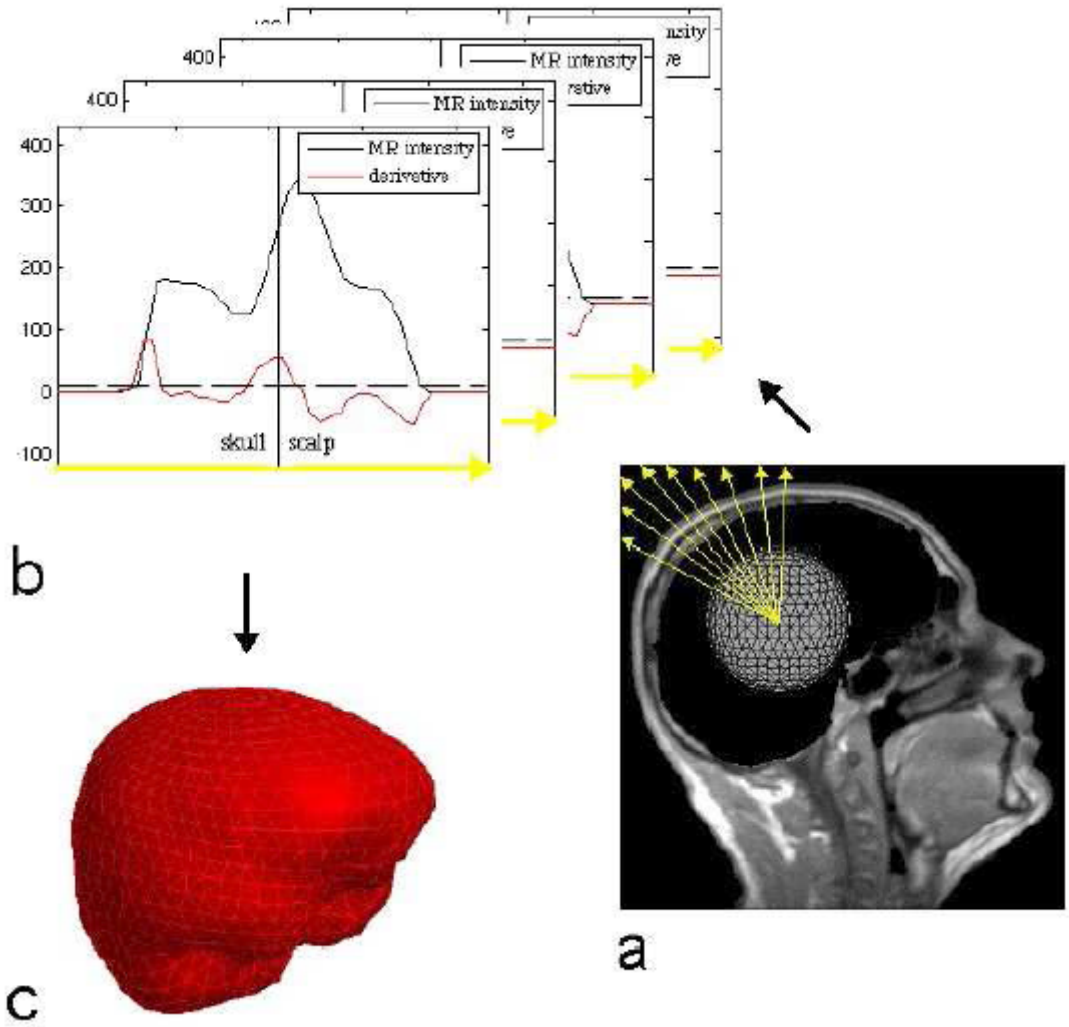

Figure 2.2: a: Evenly triangulated sphere aligned to the smoothed mri volume in a way that its centre is located at the centre of gravity of the logical brain volume. (Only one slice of the smoothed MRI volume is shown). Projection lines were drawn from the centre through the vertices of the sphere. b: For every projection line a vector was created consisting of all interpolated MRI intensity values at every 0.5 mm on the line (black line). The detection algorithm found the index of each vector that represents the skull-scalp boundary (blue line). c: All resulting coordinates form the triangulated skull surface.

process. This means we searched for the boundary between skull and scalp during the projection of the vertices of an evenly triangulated sphere to the outside direction. We developed an algorithm that automatically detects the location of this boundary by searching for local minima in the intensity values on the projection line and local maxima in the derivative of the intensity values (figure 2.2).

The triangulated brain, skull and head surfaces formed together the head model and were used for the construction of the forwardmodels that were needed for beamforming (see section 2.4.2).

2.2 Stimuli and experimental design

Tactile stimuli were presented to left and right index fingers using two piezoelectrical Braille stimulators (see figure 2.3). Each Braille stimulator had a matrix of two columns by four rows of pins

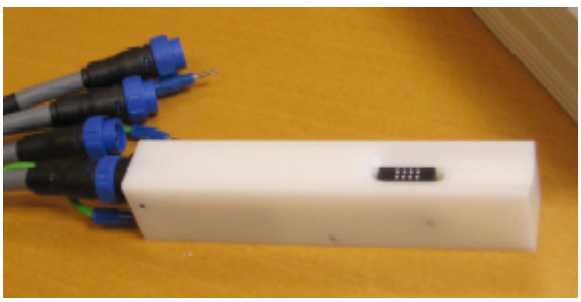

Figure 2.3: One of the piezoelectrical Braille stimulators. The stimulator contains a matrix of two columns by four rows of pins which are raised and lowered driven by a voltage.

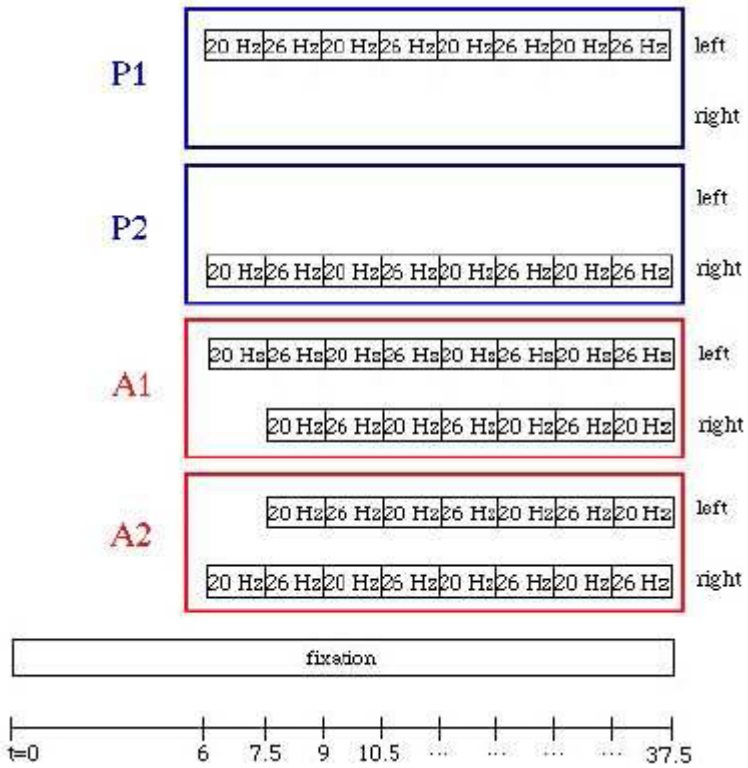

Figure 2.4: Schematic view for four different stimulus runs. P1 and P2 were perception runs in which only one index finger is stimulated by alternating 20 and 26 Hz. A1 and A2 were selective attention runs in which both index fingers are stimulated simultaneously.

which were raised and lowered all together at the same time. The vibration of the pins was driven by a block voltage. This block voltage was switched between a frequency of 20 and 26 Hz every 1.5 second.

Figure 2.4 shows a schematic view for four different stimulus runs. Every run consisted of a 6 second baseline period without tactile stimulation and a 31.5 second period with tactile stimulation. During the whole run, a cross was presented on a screen at which the subject had to fixate. In the perception runs P1 and P2, only one of the index fingers was stimulated; the left index finger in the case of P1 and the right index finger in the case of P2. In the selective attention runs A1 and A2, both index fingers were stimulated simultaneously. However, one of the tactile stimulators started vibrating 1.5 second earlier than the other. This was to indicate the finger that had to be attended. During every 1.5 second time interval of these runs, the left and right finger experienced different frequencies; i.e. 20 Hz at the left index finger and 26 Hz at the right index finger, or the other way round.

The experiment consisted of two blocks; a perception block and an attention block. The perception block included 6 P1 and 6 P2 runs which were randomly mixed. The subject was instructed to direct his attention towards the stimulated index finger. The attention block included 6 A1 and 6 A2 runs which were also randomly mixed. During these runs, the subject was instructed to direct his attention towards the index finger that was stimulated first, and ignoring the vibrations at the other finger.

In between the runs there was a small break. The start of every run was self-paced which means that the subject decided when to start the next run by pushing a button with his thumb.

2.3 Data acquisition

One of the subjects (right-handed) for which a forward model was constructed served as a volunteer in the experiment. During the experiment, the subject was sitting comfortably in a shielded room with his/her arms resting on cushions and the tips of the index fingers placed on the stimulators. To avoid any influence of the sound produced by the stimulators, pink noise was presented to the subject through headphones.

Before the experiment, the exact positions of all electrodes and of three reference points were

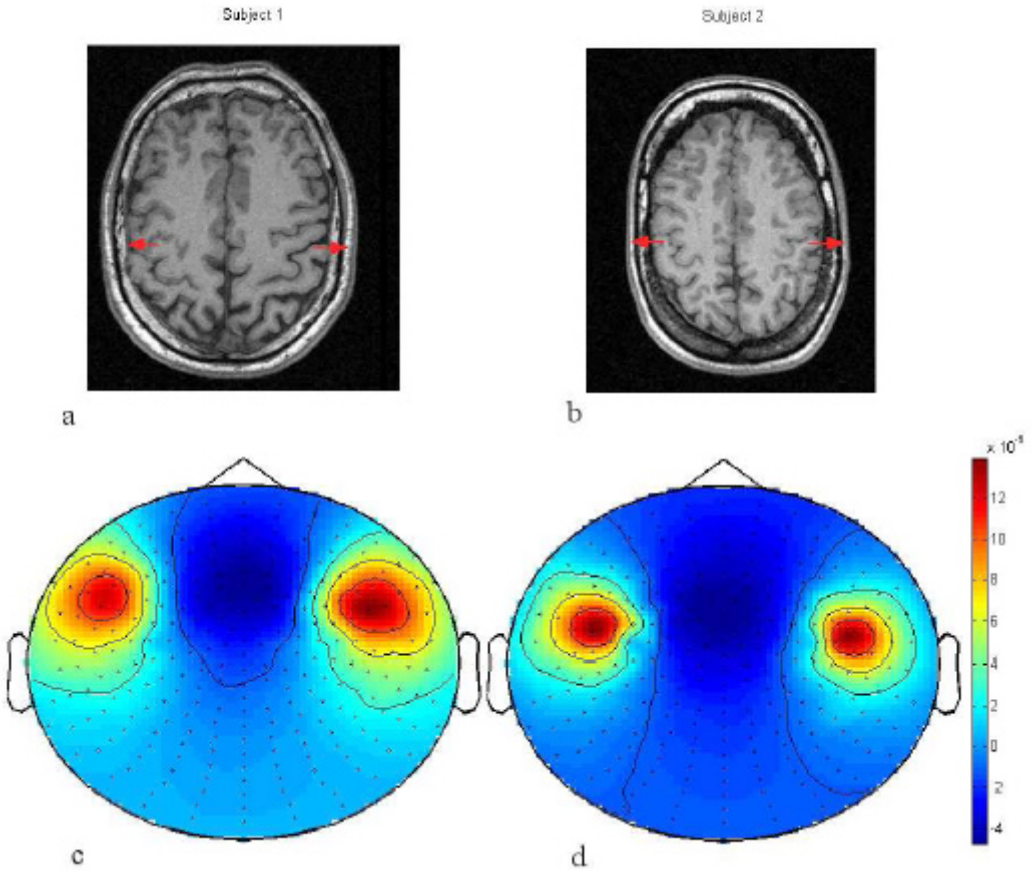

Figure 2.5: Scalp potentials simulated using the forward models for two different subjects. a and b: Two dipoles are placed into the somatosensory cortex, one is located 3.5 cm above and 4.5 cm to the left of the centre of the brain, the other is located 3.5 cm above and 4.5 cm to the right of the centre of the brain. Both dipoles have the same length, the left dipole points to left, the right dipole points to right. c and d: The scalp potentials are expressed as relative to the length of the dipoles.

measured using a magnetic tracker (MiniBIRD, Ascension Technology Corporation, Burlington). The reference points were the nasion point and the locations of the vitamin capsules in the ear plugs that the subjects wore during the making of the MRI scan.

Electrophysiological data was recorded from 256 active electrodes mounted in an elastic headcap (BIOSEMI, Amsterdam). Active electrodes and their leads are less sensitive for noise pickup than passive electrodes because the first amplifier stage is integrated in the electrodes. Eye movements and blinks were monitored by electrodes above, below, and at the sides of the eyes.

The signals were recorded with an anti-aliasing sync filter, digitized at 256 Hz and stored on a disk for offline analysis.

2.4 Data analysis

2.4.1 Alignment of electrode positions to MRI

To obtain a forward model that predicts the potentials measured by the electrodes due to sources in the brain, the positions of electrodes had to be expressed in the same coordinate system as the head model. Therefore we performed a rigid body rotation and translation on the electrode positions measured in the magnetic tracker coordinate system (cMT,i) to obtain the electrode positions in the MRI coordinate system (cMR,i):

$$cMR,i = RcMT,i + d. \quad (2.1)$$

In this equation cMR,i and cMT,i are matrices of size 3 by 1 containing the x- y- and z- coordinates of electrode i, R is a 3 by 3 rotation matrix and d is a 3 by 1 translation matrix. The rotation matrix R and translation matrix d are calculated by a least-squares fit of rigid body rotation and translation [5]. This least-squares fit was performed on the rotation and translation of the three reference coordinates from the magnetic tracker coordinates system to the MRI coordinate system. The exact coordinates of the reference points in the MRI coordinate system

Table 2.1: Sets of compared classes

comparison	class A: attention to left	class B: attention to right
1	L-20	R-26
2	L-26	R-20
3	L-20/r-26	l-20/R-26
4	L-26/r-20	l-26/R-20

were determined by examining the MRI scans in a medical image viewer (MRIcro).

2.4.2 Construction of the forward models

For every subject a forward model was constructed. This was done by applying the boundary element method (BEM) [8]. This is a numerical computational method for solving partial differential equations which is frequently used to solve field problems. The method assumes that the electrical conductivity of the head is piecewise homogeneous and requires the surfaces of all different tissue layers to be expressed as a mesh, for example as a finite number of small triangles. These meshed surfaces, the conductivity values, voxel grid and electrodes locations are then used to calculate the forward model.

In section 2.1 and appendix A is described how we constructed the meshed surfaces modeling the outside of the brain, skull and scalp. The relative conductivity values were chosen according to the research done by Oostendorp [17] and are 15:1:15, for respectively the brain, skull and scalp tissue. A three dimensional grid was constructed defining the centre coordinates of the voxels. Grid points lying outside the brain volume were removed from the grid.

The forward model was normalized in a way that the sum of potentials at all electrodes due to activity in a single voxel was zero. This was done after removing some electrodes from the model that were probably not well connected to the skin during the experiment and therefore measured signal with a very large variation. To illustrate the differences between forward models made for different subjects, in figure 2.5 the scalp potentials are simulated when two dipoles are placed into corresponding positions in different head models. The differences in surface potentials are caused by differences in the shape of brain, skull and scalp volumes between the subjects.

2.4.3 Analysis of EEG data

When using selective attention for BCI purposes, differences in EEG signals have to be found for two classes in which the presented stimuli are the same, but the attention of the subject is different. The sets of classes we compared are given in table 2.1. In the case of tactile stimulation one class can be the stimulation of the left index finger with 20 Hz, and the right index finger with 26 Hz while the subject is attending to the left index finger (L-20/r-26). The other class is than the exact same stimulation, but now the subject is attending to the right index finger (l-20/R-26). Perception classes, in which for example only the left finger is stimulated with 20 Hz (L-20) or only the right finger is stimulated with 26 Hz (R-26), are also compared as a baseline reference.

An overview of the analysis steps performed on the recorded EEG data is presented in figure 2.6. These analysis steps are performed for each set of classes. Besides the two different classes, data is analysed from the start of every run in which no tactile stimuli are given and the subject only fixates at a fixation cross. This data is used as a contrast of the stimulation data, especially for the beamformer images of brain activation during stimulation. The analysis can be divided into three parts: preprocessing and analysis of the electrode data (1-6), beamformer analysis (7-19) and classification (20-21).

Preprocessing and analysis of electrode data

Preprocessing the raw EEG data (step 1 in figure 2.6) is done using the Fieldtrip software package, a MATLAB-based toolbox (www.ru.nl/fcdonders/fieldtrip/) that is being developed by the F.C. Donders Centre (FCDC) in Nijmegen, the Netherlands. For both classes, data segments of 1.5 second were taken from the raw EEG data, starting directly after stimulus onset or after a switch in frequency. Also three data segments were

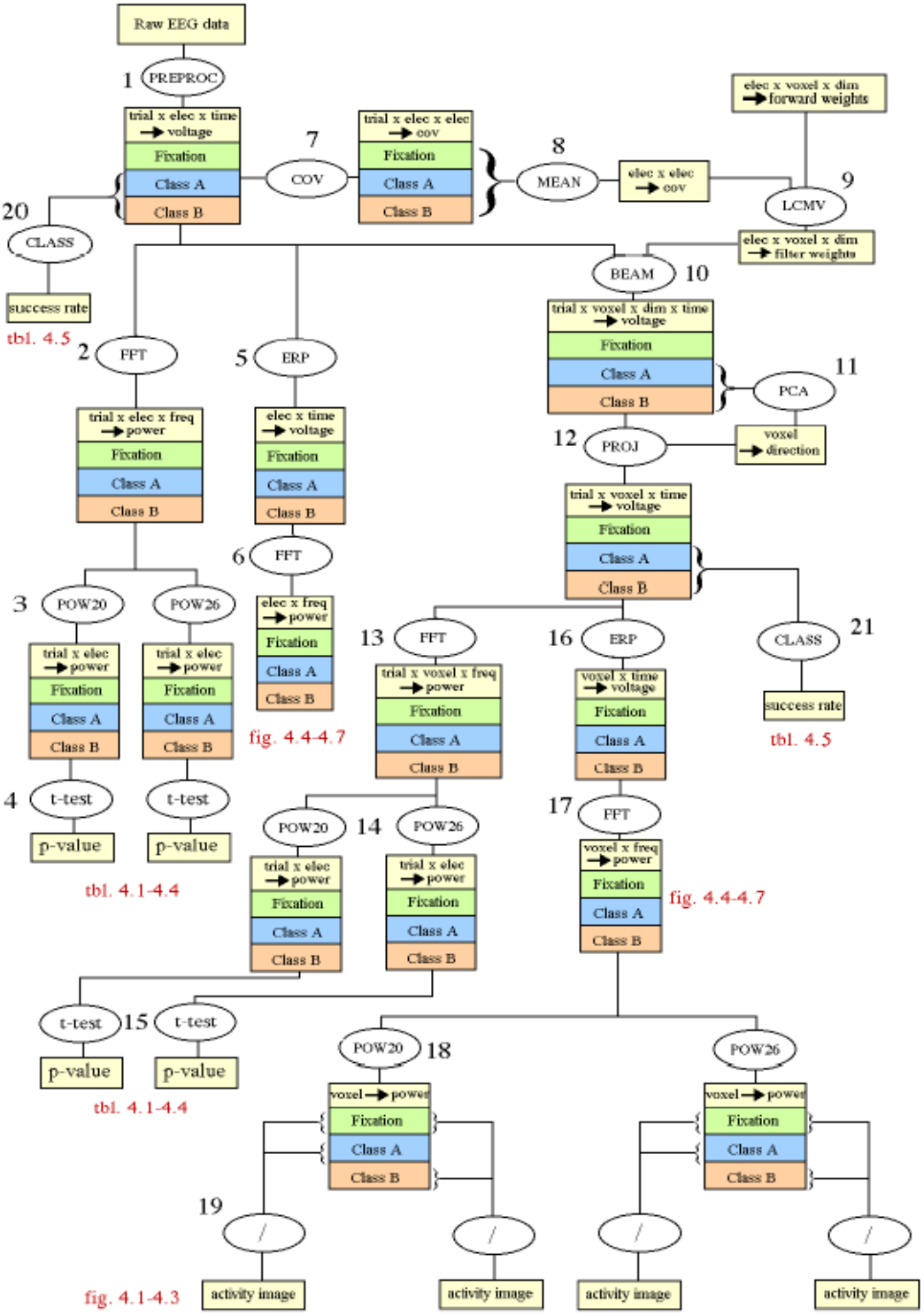

Figure 2.6: Overview of the analysis steps performed on the recorded EEG data

taken from the fixation period at the beginning of every run. These segments had also a duration of 1.5 second and started at 0.5, 2, and 3.5 seconds after onset of the fixation cross. The data segments, which are called trials, were filtered using a notch filter to remove the 50 Hz line noise. Artefacts due to eye-blinks, eye movements and muscle contractions were detected by a semi-automatic routine. This was done by determining a rejection threshold to a specific feature in the data that is sensitive for each artefact. Trials containing artefacts were removed from the set. For both classes and the fixation period data an equal amount of trials (approximately 50) was used for further analysis. All trials were baseline corrected by subtracting for every electrode the average potential over the whole duration of the trial. All data was averaged

referenced by subtracting at every moment in time the average potential of all electrodes.

Spectral analysis of the preprocessed electrode data was done in two ways. The first way was to perform a Fast Fourier Transform trial by trial (step 2 in figure 2.6), the second way was to perform a Fast Fourier Transform on the event related potential that was obtained after averaging the data over trials (step 5 and 6 in figure 2.6). In both cases, the spectrum was calculated only from the timewindow starting 0.5 second after trial onset till the end of the trial. After calculating the direct trial by trial spectra, the power at the stimuli frequencies 20 and 26 Hz of all trials was used in testing for differences between classes and differences between electrodes (step 3 and 4 in figure 2.6).

Beamformer analysis

The Linearly Constrained Minimum Variance (LCMV) method [23] was used to construct the beamformer filter. This method uses the forward model and the covariance in time between the sensor data to calculate filter weights for every voxel. This is done by minimizing the total amount of signal that can pass the filter, while ensuring that the signal expected to come from the voxel of interest is able to pass (see appendix B).

A common covariance matrix was calculated by averaging the covariance matrices for every trial of the two classes and fixation data (step 7 and 8 in figure 2.6). The filter was obtained by the LCMV method as explained in appendix B (step 9 in figure 2.6). For every trial, the electrode data was filtered using this filter (step 10 in figure 2.6). The resulting activity is expressed in an estimated x-, y-, and z-component of the dipole vector modeling the activity in the voxel. To combine these components into one single parameter for every voxel varying over time, we estimated the general direction of the dipole in every voxel and projected the x-, y- and z-components at every moment in time onto this direction vector. The estimation of the general direction of a voxel was done using Principle Component Analysis (step 11 in figure 2.6). Data from all trials of class A and class B was used to estimated the direction in which the dipole has the largest variance. The data of the classes and the fixation period was then projected in this direction to obtain a measure of the length of the dipole over time (step 12 in figure 2.6).

Spectral analysis of the voxel data was done in the same way as was done for the electrode data. A Fast Fourier Transform was performed for every trial separately (step 13 in figure 2.6) and for the event related potential (step 16 and 17 in figure 2.6). The power at the stimuli frequencies in the single trials was used in testing for differences between classes and differences between electrodes (step 14 and 15 in figure 2.6). The power at the stimuli frequencies in the event related potential was used to obtain activity images of the brain (step 18 in figure 2.6). In order to correct for the beamformer spatial bias as explained in section B.3, the power for every voxel was divided by the power calculated for the fixation period (step 19 in figure 2.6).

Classification

Both preprocessed electrode data and voxel data are used for classification (step 20 and 21 in figure 2.6). The classification scheme first combines measurements from significant channels to a limited number of features, and classifies with these features [14]. The class that gives rise to the highest posterior probability is assigned to the features, i. e. a Bayesian classifier. A multivariate normal distribution is fitted to the features per class, based on data in a training set, to calculate the posterior probability. Significant channels are extracted from the data with a cluster randomization method [15].

A cross-validation scheme was used to calculate the classification rate, because of the limited amount of data. A cross-validation scheme repeatedly divides the data into a training set and an evaluation set [10]. The training set is used to calculate the settings of the classifier, in this case the data is used to fit the normal distribution, and the evaluation set is used to estimate the classification rate. The final classification rate is the averaged value over all the individual classification rates.

3.Results

3.1 Beamformer activity images

Beamformer activity images are depicted in figures 3.1-3.3. These images are constructed by calculating for every voxel the increase in power of 20 Hz or 26 Hz in the stimulus ERP relative to the power of the same frequency in the fixation ERP. The resulting values are presented as colors on a log (dB) scale in a smoothed MRI overlay.

Figure 3.1 shows the activity for the two perception classes of comparison 1: stimulation of

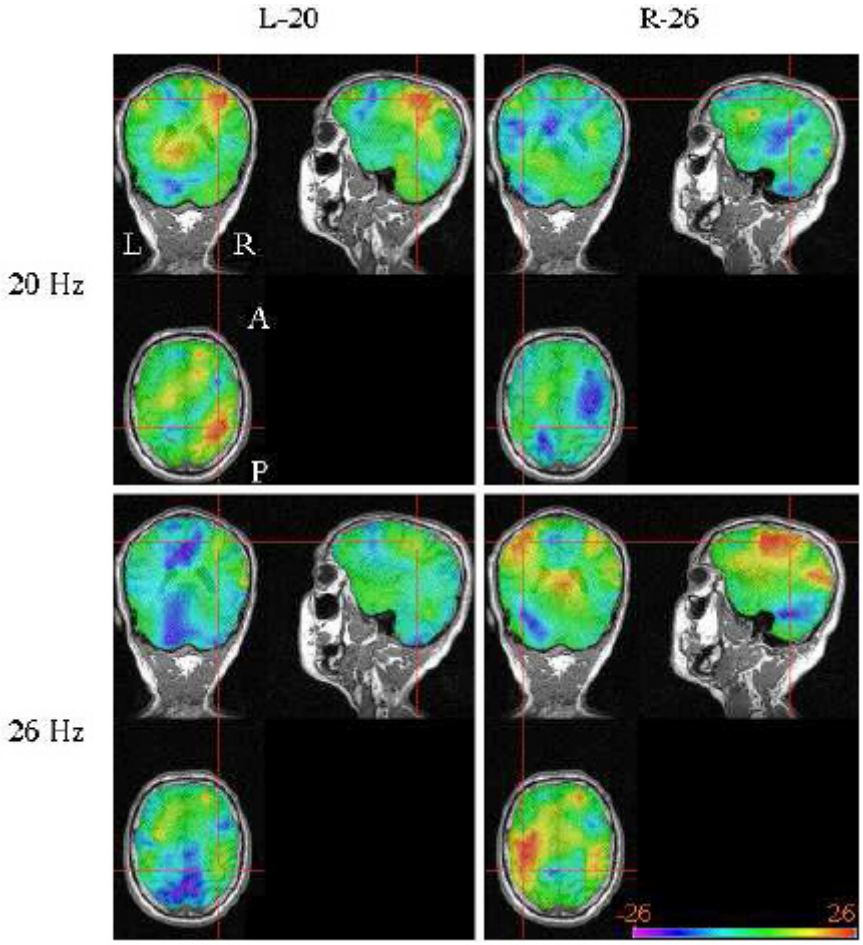

Figure 3.1: Brain activity during perception. Shown are the power increases in 20 Hz and 26 Hz for stimulation of the left index finger with 20 Hz (L-20) and stimulation of the right index finger with 26 Hz (R-26). Color indicates the dB power increase relative to the fixation period.

the left index finger with 20 Hz (L-20, left column) and stimulation of the right index finger with 26 Hz (R-26, right column). For both classes, a large increase in power for the stimulus frequency is found at the contralateral primary somatosensory cortex.

Figure 3.2 shows the activity for the two selective attention classes of comparison 3: stimulation of the left index finger with 20 Hz and the right index finger with 26 Hz while attending to the left finger (L-20/r-26, left column) and while attending to the right finger (l-20/R-26, right column). For both classes, an large increase in power is found at the contralateral primary somatosensory cortex for both stimulus frequencies. In the case of 26 Hz, this increase is visible over a large area, including parts of the temporal lobe.

Figure 3.3 shows the activity for the two perception classes of comparison 2: stimulation of the left index finger with 26 Hz (L-26) and stimulation of the right index finger with 20 Hz (R-20). The activity is also shown for the two selective attention classes of comparison 4: stimulation of the left index finger with 26 Hz and the right index finger with 20 Hz while attending to the left finger (L-26/r-20) and while attending to the right finger (l-26/R-20). Also for these classes, a large increase in power is visible in the contralateral somatosensory cortex.

All figures show brain areas where there are small decreases in 20 and 26 Hz power. The locations of these areas change per stimulus class, and might be due to measurement noise in combination with the relatively small number of trials.

3.2 Power differences between contralateral and ipsilateral channels

For both left and right hemisphere a voxel in somatosensory cortex was chosen that showed a large increase in stimulus frequency compared to the fixation period. The spectra of the ERP (step 16 and 17 in figure 2.6) for these voxels are shown

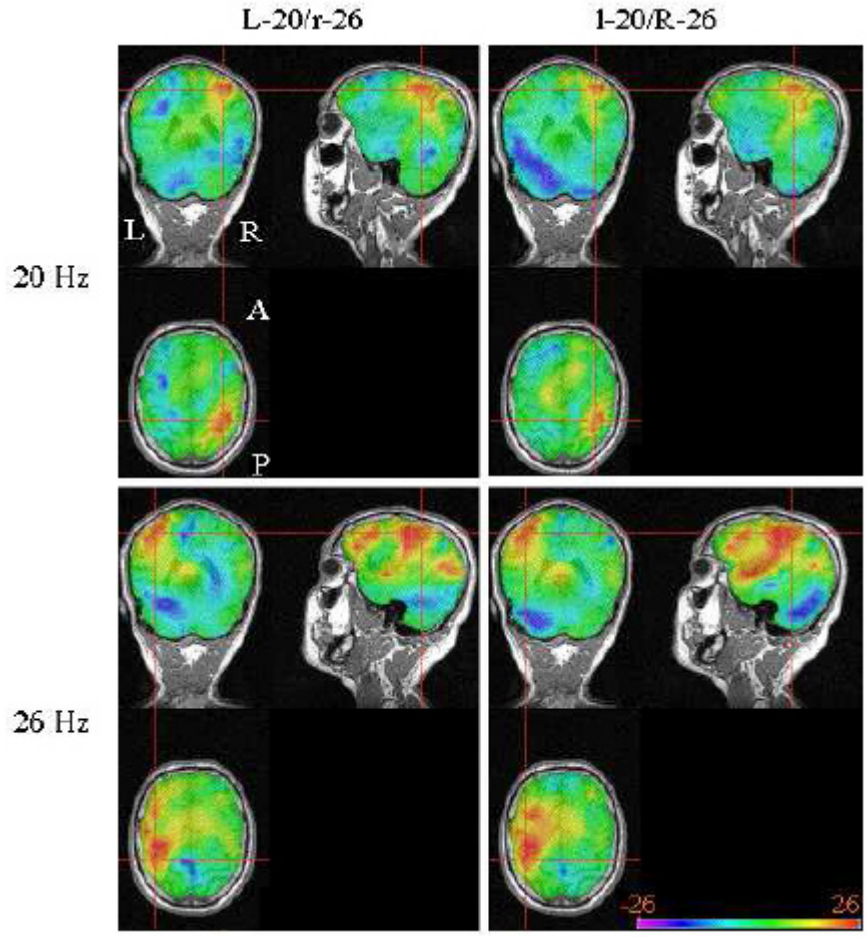

Figure 3.2: Brain activity during selective attention. Shown are power increases in 20 Hz and 26 Hz for stimulation of the left index finger with 20 Hz and right index finger with 26 Hz while attending to the left index finger (L-20/r-26) and while attending to the right index finger (l-20/R-26). Color indicates the dB power increase relative to the fixation period.

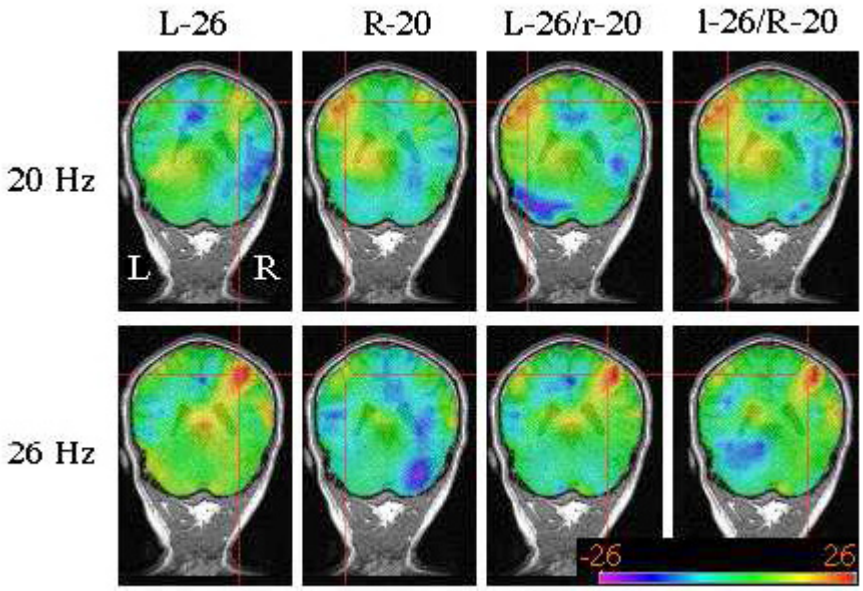

Figure 3.3: Shown are power increases in 20 Hz and 26 Hz for the conditions L-26, R-20, L-26/r-20 and l-26/R-20. Color indicates the dB power increase relative to the fixation period.

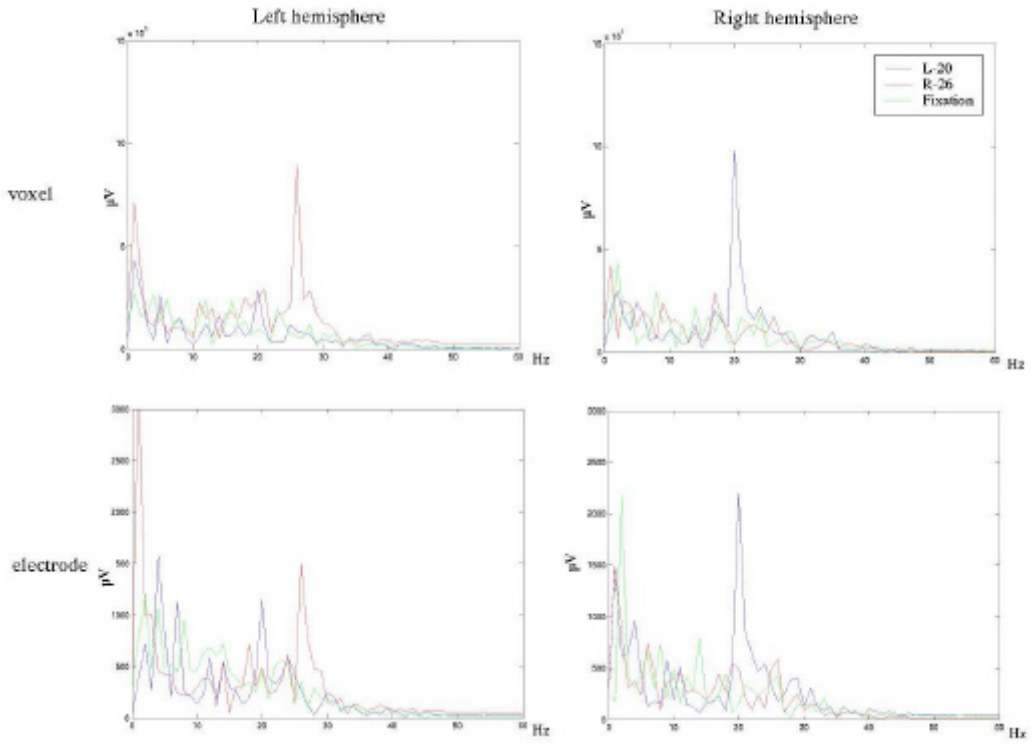

Figure 3.4: Spectra of the ERP measured by two voxels and two electrodes in the case of stimulation of the left finger with 20 Hz (blue), stimulation of the right finger with 26 Hz (red) or when there is no stimulation (green). Electrodes and voxels were located in and above somatosensory cortex in left and right hemisphere.

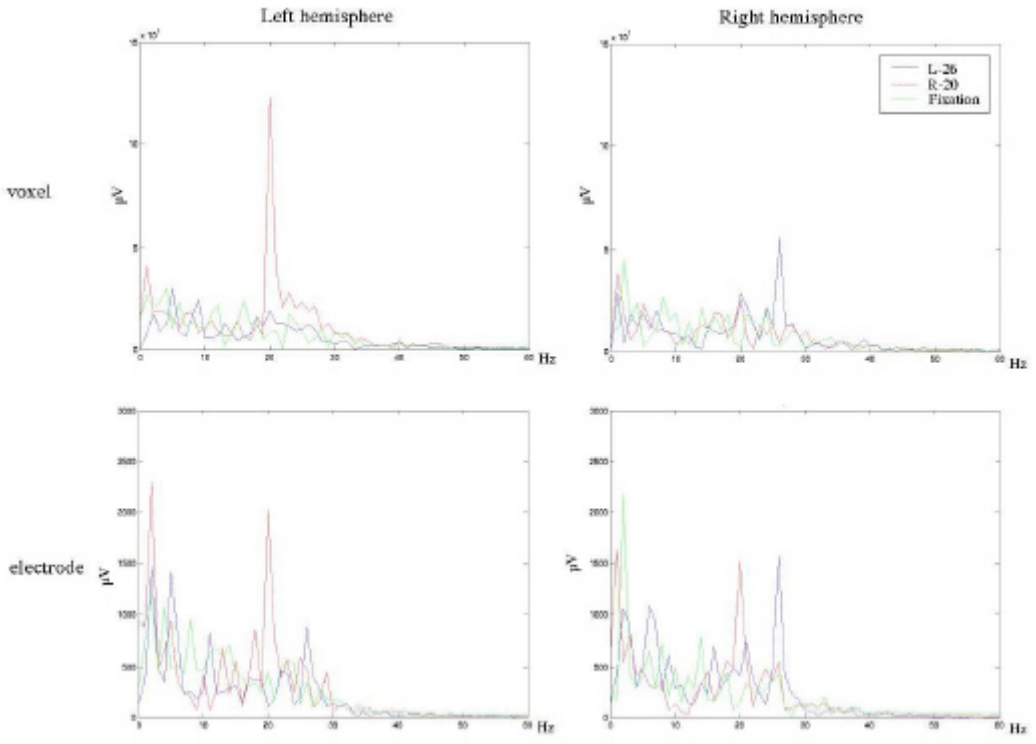

Figure 3.5: Spectra of the ERP measured by two voxels and two electrodes in the case of stimulation of the left finger with 26 Hz (blue), stimulation of the right finger with 20 Hz (red) or when there is no stimulation (green).

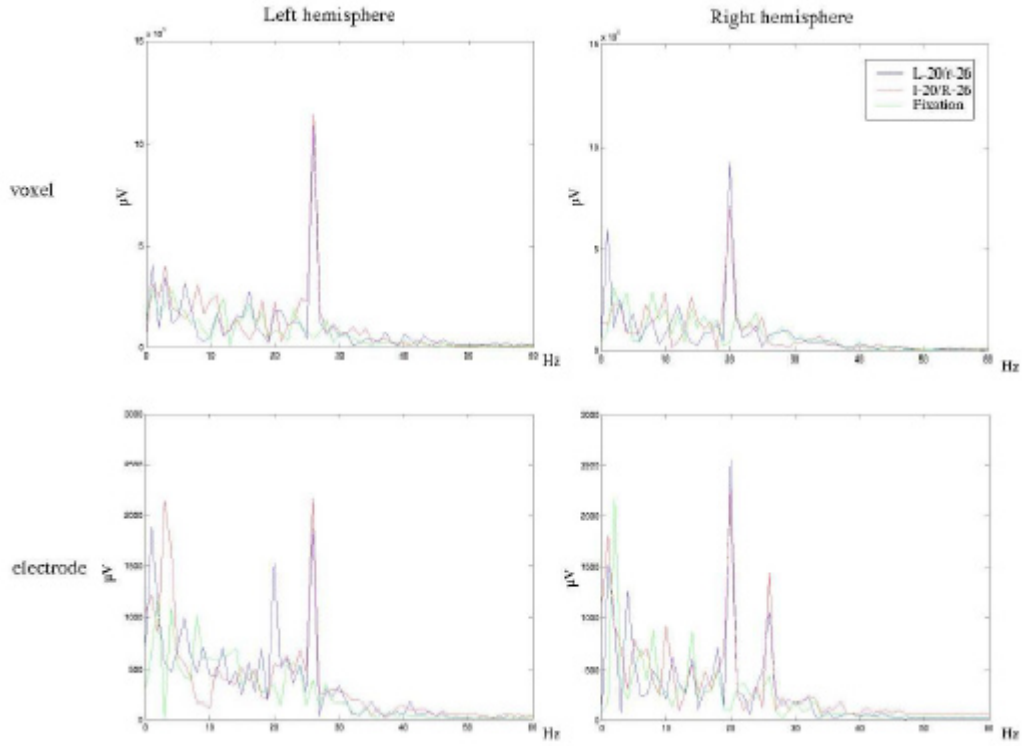

Figure 3.6: Spectra of the ERP measured by two voxels and two electrodes in the case of stimulation of the left finger with 20 Hz and the right finger with 26 Hz while attention was to the left finger (blue), and while attention was to the right finger (red). The spectrum is also shown for the the case when there is no stimulation (green).

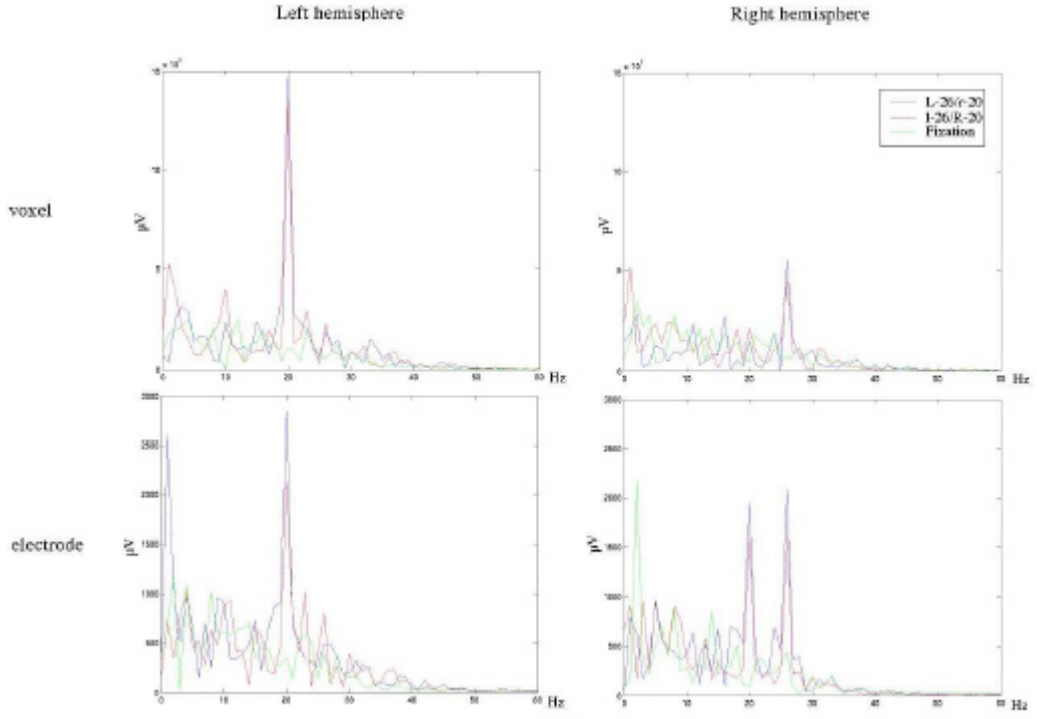

Figure 3.7: Spectra of the ERP measured by two voxels and two electrodes in the case of stimulation of the left finger with 26 Hz and the right finger with 20 Hz while attention was to the left finger (blue), and while attention was to the right finger (red). The spectrum is also shown for the the case when there is no stimulation (green).

Table 3.1: Power change in ERP between contralateral and ipsilateral channels(dB)

	voxel		electrode	
Stimulus	20 Hz	26 Hz	20 Hz	26 Hz
L-20	10.7		5.6	
R-20	13.7		2.5	
L-26		12.9		4.9
R-26		14.1		8.1
L-20/r-26	14.2	23.6	4.5	4.9
l-20/R-26	10.1	29.8	12.2	3.5
L-26/r-20	20.4	9.7	3.2	12.5
l-26/R-20	16.3	6.1	2.5	5.9

Table 3.2: Significance of differences between contralateral and ipsilateral channels

	voxel		electrode	
Stimulus	20 Hz	26 Hz	20 Hz	26 Hz
L-20	<0.0001*		0.06	
R-20	<0.0001*		0.0006*	
L-26		0.01*		0.04*
R-26		<0.0001*		0.01*
L-20/r-26	0.03*	<0.0001*	0.5	0.0002*
l-20/R-26	0.01*	<0.0001*	0.4	0.004*
L-26/r-20	<0.0001*	0.1	0.0002*	0.2
l-26/R-20	<0.0001*	0.2	<0.0001*	0.4

in the first rows of figures 3.4-3.7. The second rows in these figures show the spectra of the ERP for two electrodes above the left and right hemisphere that are expected to measure the largest potential differences when left or right somatosensory cortex is active. These electrodes were chosen by simulating the scalp potentials when a dipole was placed at the location of the chosen voxels pointing into the direction of the activity (calculated in step 11 of figure 2.6).

Figures 3.4 and 3.5 show the spectra of the perception classes of comparison 1 and 2. The voxel spectra show clear peaks for the stimulus frequency that is presented to the contralateral finger, for example 20 Hz for the voxel in the right hemisphere in the case of L-20, and 26 Hz for the voxel in the left hemisphere in the case of R-26. When looking at the frequency that is presented to the ipsilateral finger, no clear peaks are detected. The electrode spectra show peaks at the same frequencies as the voxel spectra. However, the stimulation frequency is not only found in the contralateral electrode, but peaks are also found at the ipsilateral electrode, for example a peak at 20 Hz for the left electrode in the case of L-20.

In table 3.1 the power change of the stimuli frequencies in the erp between contralateral and ipsilateral channels are shown. These power changes are expressed in dB change for the power in the stimuli frequency found contralateral to the stimulus side compared to the power found ipsilateral to the stimulus side. The stimulus side is defined as the side at which the finger is stimulated at the specified frequency. The comparison is made between the same voxels and electrodes used for figures 3.4-3.7. All values in table 3.1 are positive which means that the frequency power at the contralateral channel is always larger than the frequency power at the ipsilateral channel. Furthermore, the gain between contralateral and ipsilateral voxels (on average 12.9 dB for perception and 16.3 dB for selective attention) is in most cases larger than the gain between contralateral and ipsilateral electrodes (on average 5.3 dB for perception and 6.2 dB for selective attention). The only exceptions to this are 20 Hz in stimulus l-20/R-26 and 26 Hz in stimulus

Table 3.3: Attention induced power change in ERP (dB)

	voxel				electrode			
	contralateral		ipsilateral		contralateral		ipsilateral	
Stimulus	20 Hz	26 Hz	20 Hz	26 Hz	20 Hz	26 Hz	20 Hz	26 Hz
L-20 vs. R-26	29.1	20.5	1.1	4.7	12.9	15.0	7.4	10.5
L-26 vs. R-20	16.1	23.3	-0.9	-3.6	25.0	9.1	11.3	5.6
L-20/r-26 vs. l-20/R-26	2.3	0.4	-1.9	-5.8	1.1	1.3	8.8	2.7
L-26/r-20 vs. l-26/R-20	-1.0	1.9	3.1	-1.8	-2.5	2.4	-1.8	-4.3

Table 3.4: Significance of differences between conditions

	voxel				electrode			
	contralateral		ipsilateral		contralateral		ipsilateral	
Stimulus	20 Hz	26 Hz	20 Hz	26 Hz	20 Hz	26 Hz	20 Hz	26 Hz
L-20 vs. R-26	<0.0001*	<0.0001*	0.4	0.4	<0.0001*	0.0006*	0.2	0.1
L-26 vs. R-20	<0.0001*	0.001*	0.4	0.1	0.0001*	0.008*	0.01*	0.04*
L-20/r-26 vs. l-20/R-26	0.3	0.4	0.2	0.5	0.3	0.9	0.3	0.4
L-26/r-20 vs. l-26/R-20	0.8	0.2	0.9	0.4	0.9	0.1	0.7	0.4

L-26/r-20.

In table 3.2 significance values of power differences between contralateral and ipsilateral channels are shown. These values were calculated by performing Student t-tests between the stimulus frequency power in the contralateral and ipsilateral channel in every trial separately (step 13 and 14 in figure 2.6). For voxels, we found significant differences for almost all stimuli and frequencies (10 of 12 t-tests gave p-values lower than 0.05). For electrodes, only 7 of 12 t-tests gave significant results. In general, significance values for voxel data were lower than for electrode data. This means that in voxel data the stimulation frequencies given to the left and the right index finger are more concentrated to separate areas of the brain than in electrode data.

3.3 Attention induced power change

In table 3.3 the attention induced power change in the ERP is shown when comparing the power for the stimulus frequency between attention to the left index finger and attention to the right index finger. These power changes are expressed in dB change for the case the finger experiencing the specified frequency is attended compared to the case that the finger is not attended. For example, in the cases when the left finger is stimulated with 20 Hz and the right finger with 26 Hz (L-20/r-26 and l-20/R-26) the voxel contralateral to the 20 Hz stimulation (the voxel in the right hemisphere) shows a 2.3 dB power increase when the left finger is attended (L-20/r-26) compared to when the right finger is attended (l-20/R-26). The voxel contralateral to the 26 Hz stimulation (the voxel in the left hemisphere) shows a 0.4 power increase when the right finger is attended (l-20/R-26) compared to when the left finger is attended (L-20/r-26). For the perception classes, contralateral voxels and electrodes show a large attention induced power change when the finger stimulated with the frequency is attended, compared to when the other finger is attended. This is also expected, because only the attended finger is stimulated and in the compared class the other finger is stimulated at another frequency. Furthermore, the increase in power is larger for the contralateral voxel (on average 22.3 dB) than for the contralateral electrode (on average 15.5 dB) in 3 of the 4 comparisons. For ipsilateral voxels, the increase in frequency power is smaller (on average 0.33 dB) than for ipsilateral electrodes (on average 8.7 dB) and in two cases there is even a decrease in power. For the attention classes, contralateral voxels and electrodes show a small increase in stimulus frequency power when the finger is attended in 3 of the 4 comparisons.

In table 3.4 significance values of differences between conditions are shown. These values were calculated by performing Student t-tests between the stimulus frequency power for every condition in every trial separately (step 13 and 14 in figure 2.6). The significances are calculated for both contralateral and ipsilateral voxels and electrodes. For perception classes, there is a significant increase in stimulus frequency power in the voxels contralateral to the side of the stimulated finger. The same is the case for contralateral electrodes although the significance is slightly larger. Ipsilateral voxels do not show a significant increase in

Table 3.5: Classification success rates

Stimulus	voxel data	electrode data
L-20 vs. R-26	0.88	0.90
L-26 vs. R-20	0.87	0.91
L-20/r-26 vs. l-20/R-26	0.42	0.41
L-26/r-20 vs. l-26/R-20	0.49	0.39

frequency power, while in two cases ipsilateral electrodes do show a significant increase. For attention classes no significant increases are found.

3.4 Classification success rates

In table 3.5 the success rates are given for classification. For the perception classes both voxel and electrode data give very large success rates. For these classes, the success rates of the electrode data are slightly larger than that of the voxel data. Selective attention classes give for both voxel and electrode data very small success rates, even below change level.

4.Discussion

The aim of the experiment described in this thesis was to explore the possibility to elaborate a new type of BCI system: a system in which selective attention to temporal rhythmic stimuli is used to control an external device. Simultaneously, beamformer techniques were used to see if the success rates of the classification procedure would improve. To be sure that the beamformer filter allocates activity to the correct anatomical locations, a new method was proposed to construct realistic head models.

When looking at the power of the stimulus frequencies in the ERP, a clear increase was found in the somatosensory cortex contralateral to the stimulus side compared to the fixation period. This corresponds to the steady-state somatosensory evoked potentials found in [12] [13] [21]. This finding means that the beamformer filter based on the realistic head model is able to allocate the measured EEG activity to brain areas in an accurate way.

For both voxel and electrode channels the power in the contralateral channel is larger than the power in the ipsilateral channel, but the gain in power is larger for voxel data than for electrode data. Furthermore, the significance values for differences between these channels in single trials are also smaller for voxel data. These findings indicate that beamforming allocates the different stimulation frequencies to separate areas of the brain, while the frequencies found in the original electrode data reach both sides of the scalp. By this spatial separation of frequencies the power of a single stimulus is focused to a single area which will increase the signal to noise ratio. Therefore, signals allocated to voxels in these areas might give a more accurate estimation of the power of the steady-state somatosensory evoked potential than electrode signals.

For both contralateral voxel and electrode channels an increase in power is found between the compared perception classes. This increase is larger for voxel channels, which confirms the idea that voxel data has a larger signal to noise ratio. The attention induced power gain calculated from the data measured in the selective attention conditions is small and not significant present in single trials.

Perception success rates are relatively high when voxel or electrode data is used in the classification algorithm. Success rates for electrode data are slightly larger than for voxel data. An explanation can be that cross talk between some electrodes and the stimulator leads results in a large power for the stimulation frequency in some electrode signals. If this happens at isolated electrodes, beamforming will ignore the signals because they are not correlated with the signals from neighbouring electrodes. Classification success rates for selective attention classes are very low and even below chance level. Probably the signal to noise level of the attention induced power gain is too small to be measured in single trials and averaging over a few trials is necessary. Recently, a new classification algorithm is developed that uses the features of two successive trials for classification. This algorithm gives higher classification success rates ($\pm$ 60%). Probably influences in frequency power due to other ongoing brain processes are reduced by using also the power during the second trial in which the frequencies are switched.

An important suggestion for improving the experiment is to include a period in each run in which the stimulators are active, but the fingers of

the subject are not attached. The vibrating of the stimulators should be the same as the experiment, and the subject should be fixating to a fixation cross during the stimulation. The data recorded during this time period can then be used as a baseline instead of the fixation baseline. In this way the probability that differences between stimulation and baseline are the result of crosstalk is reduced. This baseline data can also be used in the classification algorithm to see if the success rates are (partially) due to cross talk. Next, a discrimination task can be added to the experiment, for example the task to detect a small interruption in time of the stimulus at the attended side while ignoring the interruptions at the not attended side. This might increase the attention level of the subject and therefore the attention induced power gain. Furthermore, it might be worthwhile to examine if other tactile stimuli, for example stimuli without alternating frequencies give better results.

A suggestion for improving the analysis of the experimental data is to increase the amount of trials that is used as a training set in the cross validation procedure. This can be done by combining the data from multiple experiment sessions. The beamformer filter could be improved by using more trials in estimating the covariance matrix. If the data analysis can be performed online, i.e. during the experiment, direct feedback about the chosen class can be given to the subject. This might encourage the subject to concentrate and might increase the attention induced power gain. Furthermore it might be necessary to use the average signal over a small amount (2-3) of trials to increase the signal to noise ratio. However, this will increase the time needed for every decision and therefore slows down the system.

Further research will show if the results described in this thesis are representative to the results of experiments with other subjects. More analysis should be done to investigate if beamforming gives better results than other spatial filters like independent component analysis (ICA). Furthermore, a comparison can be made between the beamformer results obtained when the forward model is based on a simple sphere model to the results obtained when it is based on the realistic head models we constructed.

References

[1] J. Ashburner and K.J. Friston, "Multimodal Image Coregistration and Partitioning - a Unified Framework," NeuroImage., vol. 6(3), pp. 209-217, 1997.

[2] N. Birbaumer, T. Elbert, A.G.M. Canavan, and B. Roch,"Slow potentials of the cerebral cortex and behavior," Physiological Reviews., vol. 70, pp.1-41, 1990.

[3] N. Birbaumer, A. Kubler, N. Ghanayim, T. Hinterberger, J. Perelmouter, J. Kaiser, I. Iversen, B. Kotchoubey, N. Neumann, and H. Flor,"The thought translation device (TTD) for completely paralyzed patients." IEEE Transactions on Rehabilitation Engineering., vol. 8, pp. 190-192, 2000.

[4] J.M. Carmena, M.A. Lebedev, R.E. Crist, J.E. O' Doherty, D.M. Santucci, D.F. Dimitrov, P.G. Patil, C.S. Henriquez, and M.A. Nicolelis,"Learning to control a brain-machine interface for reaching and grasping by primates," PLoS Biol., vol. 1(2): e2, 2003.

[5] J.H. Challis,"A prodecure for determining rigid body transformation parameters," Journal of Biomechanics., vol. 28, pp. 733-737,1995.

[6] L.A. Farwell, and E. Donchin, "Talking off the top of your head: toward a mental prothesis utilizing event-related brain potentials," Electroencephalography and Clinical Neurophysiology., vol. 70, pp. 510-523, 1988.

[7] E.E. Fetz, and M.A. Baker, "Operantly conditioned patterns on precentral unit activity and correlated responses in adjacent cells and contralateral muscles," Journal of Neurophysiology., vol. 36(2), pp. 179-204, 1973.

[8] M. Fuchs, J. Kastner, M. Wagner, S. Hawes, and J.S. Ebersole, "A standardized boundary element method volume conductor model," Clinical Neuropfysiology., vol. 113(5), pp. 702-712, 2002.

[9] C.M. Giabbiconi, C. Dancer, R. Zoph, T. Gruber, and M.M. Muller, "Selective spatial attention to left or right hand flutter sensation modulates the steady-state somatosensory evoked potential," Cognitive Brain Research., vol. 20, pp. 58-66, 2004.

[10] S. Haykin, "Neural Networks, a comprehensive foundation," Upper Saddle River, New Jersey: Prentice Hall, 1999.

[11] A. Hillebrand, K.D. Singh, I.E. Holliday, P.L. Furlong, and G.R. Barnes, "A New Approach to Neuroimaging With Magnetoencephalography," Human Brain Mapping., vol. 25, pp. 199-211, 2005.

[12] E.F. Kelly, and S.E. Folger,"EEG evidence of stimulus-directed response dynamics in human somatosensory coretex," Brain Research., vol. 815, pp. 326-336, 1999.

[13] E.F. Kelly, M. Trulsson, and S.E. Folger,"Periodic microstimulation of single mechanoreceptive afferents produces frequency-following responses in human EEG," Journal of Neurophysiology., vol. 77, pp. 137-144, 1997.

[14] B.J. de Kruif, P. Desain, and C.C.A.M. Gielen, "Combining multiple sensors and measurements to improve frequency tagged BCI," to be submitted

[15] E. Maris, "Randomization tests for erp topographies and whole spatiotemporal data matrices,"

Psychophysiology., vol. 41, pp. 142-151, 2004.
[16] S. Musallam, B.D. Corneil, B. Greger, H. Scherberger, and R.A. Andersen,"Cognitive control signals for neural prosthetics," Science., vol. 305, pp. 258-262, 2004.
[17] T.F. Oostendorp, J. Delbeke and D.F. Stegeman, "The Conductivity of the Human Skull; Results of In Vivo and In Vitro Measurements," IEEE Transactions on Biomedical Engineering., vol. BME-47, pp. 1487-1492, 2000.
[18] G. Pfurtscheller, B. Graimann, J.E. Huggins, S.P. Levine, and L.A. Schuh,"Spatiotemporal patterns of beta desynchronization and gamma synchronization in corticographic data during self-paced movement," Clinical Neuropfysiology., vol. 114(7), pp. 1226-1236, 2003.
[19] G. Pfurtscheller, C. Neuper, G.R. Muller, B. Obermaier, G. Krausz, A. Schlogl, R. Scherer, B. Graimann, C. Keinrath, D. Skliris, M. Wortz, G. Supp, and C. Schrank,"Graz-BCI: state of the art and clinical applications," IEEE Transactions on Neural Systems and Rehabilitation Engineering., vol. 11(2), pp. 177-180, 2003.
[20] E.M. Schmidt, "Single neuron recording from motor cortex as a possible source of signals for control of external devices," Annals of Biomedical Engineering., vol. 8, pp. 339-349, 1980.
[21] S. Tobimatsu, Y.M. Zhang, and M. Kato, "Steady-state vibration somatosensory evoked potentials: physiological characteristics and tuning function," Clinical Neuropfysiology., vol. 110, pp. 1953-1958, 1999.
[22] B. Vanrumste, G. Van Hoey, R. Van deWalle, M.R. D' Have, I.A. Lemahieu, and P.A.. Boon, "Comparison of performance of spherical and realistic head models in dipole localization from noisy EEG," Med Eng & Phys., vol. 24, pp. 403-418, 2002.
[23] B.D. Van Veen, W. van Drongelen, M. Yuchtman, and A. Suzuki, "Localization of Brain Electrical Activity via Linearly Constrained Minimum Variance Spatial Filtering," IEEE Transactions on Biomedical Engineering., vol. 44(9), pp. 867-880, 1997.
[24] J. Wessberg, C.R. Stambaugh, J.D. Kralik, P.D. Beck, M. Laubach, J.K. Chapin, J. Kim, S.J. Biggs, M.A. Srinivasan, and M.A. Nicolelis, "Real-time prediction of hand trajectory by ensembles of cortical neurons in primates," Nature., vol. 408, pp. 361-365, 2000.
[25] J.R. Wolpaw, N. Birbaumer, D.J. McFarlanda, G. Pfurtschellere, and T.M. Vaughana, "Brain computer interfaces for communication and control," Clinical Neuropfysiology., vol. 113, pp. 767-791, 2002.
[26] F.C. Donders Centre for Cognitive Neuroimaging, Nijmegen, The Netherlands